Developmental Cell, Vol. 2, 477–488, April, 2002, Copyright ©2002 by Cell Press

Insulin Causes Fatty Acid Transport Protein Translocation and Enhanced Fatty Acid Uptake in Adipocytes

Andreas Stahl,[1,4] James G. Evans,[1] Shraddha Pattel,[1] David Hirsch,[1] and Harvey F. Lodish[1,2,3]
[1]Whitehead Institute for Biomedical Research
9 Cambridge Center
Cambridge, Massachusetts 02142
[2]Department of Biology
Massachusetts Institute of Technology
Cambridge, Massachusetts 02139

Summary

Fatty acid uptake into 3T3 L1 adipocytes is predominantly transporter mediated. Here we show that, during 3T3 L1 adipocyte differentiation, expression of fatty acid transport proteins (FATPs) 1 and 4 is induced. Using subcellular membrane fractionation and immunofluorescence microscopy, we demonstrate that, in adipocytes, insulin induces plasma membrane translocation of FATPs from an intracellular perinuclear compartment to the plasma membrane. This translocation was observed within minutes of insulin treatment and was paralleled by an increase in long chain fatty acid (LCFA) uptake. In contrast, treatment with TNF-α inhibited basal and insulin-induced LCFA uptake and reduced FATP1 and -4 levels. Thus, hormonal regulation of FATP activity may play an important role in energy homeostasis and metabolic disorders such as type 2 diabetes.

Introduction

Under normal conditions more than 95% of total body triglyceride is sequestered in adipocytes, which are approximately 80% triglyceride by weight. Free long chain fatty acids (LCFAs) are formed in the circulation through the action of lipases and are bound to albumin; LCFAs are imported into adipocytes and esterified to glycerol, forming triglycerides.

Levels of both glucose and LCFAs in the circulation rise after a meal (Frayn, 1998). High postprandial glucose levels are counteracted by insulin, which reduces gluconeogenesis in the liver and increases glucose uptake predominantly into skeletal muscle (Cherrington, 1999; Kahn, 1996). Similarly, LCFA blood levels decrease in response to insulin, but it has been unclear whether this is also due to a combination of decreased release and increased uptake. Insulin can potentially affect the generation of LCFAs from triglycerides in adipose tissue by inhibiting catecholamine-induced lipolysis through phosphorylation and activation of phosphodiesterase 3B, leading to decreased cAMP levels, which prevent the activation of hormone-sensitive lipase (Holm et al., 2000). How insulin affects the uptake of LCFAs has not been studied extensively.

Uptake of LCFAs into adipocytes is predominantly a transporter-mediated process, with more than 90% occurring via a saturable pathway (Stump et al., 2001). Several proteins have been suggested to mediate fatty acid uptake by adipocytes, including intracellular molecules such as fatty acid binding proteins (FABP), long chain fatty acyl-CoA synthases (LACS), and adipose differentiation-related protein (ADRP). Indeed, overexpression of LACS or ADRP in COS cells increases fatty acid uptake (Gao et al., 2000; Schaffer and Lodish, 1994). By lowering the intracellular concentration of free fatty acids, these proteins facilitate the movement of fatty acids into the cell.

Substantial evidence indicates that two plasma membrane proteins, FAT/CD36 and FATP1, facilitate uptake of LCFAs. Both increase fatty acid uptake when overexpressed in cell lines, and FAT/CD36 and FATP1 are strongly induced when fibroblast cell lines are differentiated into adipocytes (this paper; Abumrad et al., 1991). Adipocytes from FAT/CD36 knockout mice have a reduced ability to take up fatty acids at low fatty acid to albumin ratios (Coburn et al., 2001). Recently we have shown that FATP1 is part of a large evolutionarily conserved gene family (Stahl et al., 2001). Mammals have six homologs, designated FATP1–6, and highly homologous genes are found in other organisms, including flies, worms, fish, and yeast. FATP1 is expressed in brain, skeletal muscle, heart, fat, and kidney, but not in liver. FATP2 is expressed exclusively in liver and kidney, and FATP5 is expressed only in adult liver (Hirsch et al., 1998). FATP4 is expressed predominantly in the small intestine; it is localized specifically to the brush border of the absorptive epithelial cells and is essential for uptake of LCFAs by these cells (Stahl et al., 1999).

Insulin increases glucose uptake into muscle and other target tissues by stimulating the translocation of the glucose transporter Glut4 from an intracellular pool to the plasma membrane (Kahn, 1996). Here we show that insulin causes a similar translocation of FATPs in adipocytes and induces an increase in fatty acid uptake, suggesting that hormonal regulation of FATP activity may play an important role in energy homeostasis.

Results

Fatty Acid Uptake and FATP Expression Are Induced during 3T3 L1 Differentiation

During differentiation, 3T3 L1 cells change from fibroblast-like progenitors to lipid-accumulating adipocytes. We compared the LCFA uptake properties of fibroblasts and adipocytes by measuring the initial uptake velocities of the water-soluble naturally occurring LCFA *cis*-parinaric acid at different concentrations (Fraser et al., 1997). LCFA uptake into adipocytes in the concentration range of 0.1–10 μM *cis*-parinaric acid was approximately

[3]Correspondence: lodish@wi.mit.edu
[4]Present address: Research Institute, Palo Alto Medical Foundation, 795 El Camino Real, Palo Alto, California 94301 and Division of Gastroenterology and Hepatology, Stanford University School of Medicine, CCSR Building, Room 3115, 269 Campus Drive, Stanford, California 94305.

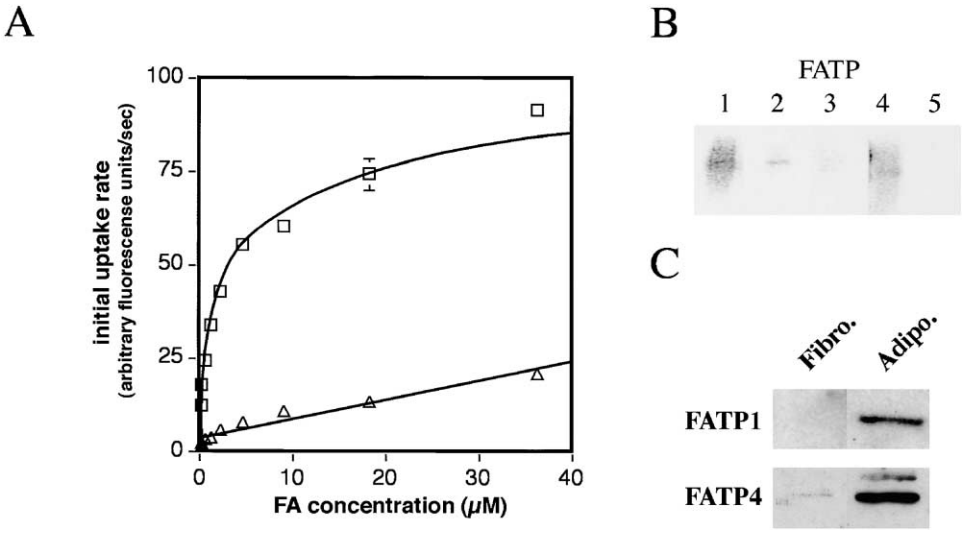

Figure 1. LCFA Uptake and FATP Expression of 3T3 L1 Fibroblasts and Adipocytes

(A) Initial LCFA rates of uptake into 3T3 L1 fibroblasts (triangles) or differentiated 3T3 L1 adipocytes (squares) were measured in triplicate using *cis*-parinaric acid at the given concentrations. Linear and logarithmic curve fits are shown for fibroblasts and adipocytes, respectively.

(B) Northern blot of poly(A)$^+$ mRNA from mouse adipocytes hybridized with specific probes for either FATP1, -2, -3, -4, or -5 of similar specific activity and exposed for identical amounts of time.

(C) Western blot of FATP1 and -4 proteins. Equal amounts of lysates (25 μg/lane) from 3T3 L1 fibroblasts or adipocytes were separated by denaturing gel electrophoresis on 8%–16% acrylamide gradient gels, blotted onto nitrocellulose, and probed with antibodies for either FATP1 or -4.

10-fold higher than into fibroblasts (Figure 1A). LCFA uptake into adipocytes was saturable at higher concentrations of *cis*-parinaric acid, indicative of protein-mediated uptake, while LCFA uptake into fibroblast showed a linear concentration dependency as expected from a process predominantly based on diffusion (Figure 1A).

Northern blot analysis using FATP-specific probes with comparable specific activity showed that mature adipocytes mainly express FATP1; at lower levels they express FATP4, and at very low levels they express FATP2 (Figure 1B). To see whether FATP expression changes during 3T3 L1 differentiation, equal amounts of protein from fibroblasts and adipocytes were blotted and probed with polyclonal anti-sera specific for either FATP1 or -4. Both proteins are induced during differentiation, as they are absent in preadipocytes but robustly expressed in adipocytes (Figure 1C). Note that the stronger signal in the FATP4 lane does not reflect a higher expression level of FATP4 over FATP1 but is due rather to differences in the sensitivity of the anti-sera. None of the other four FATPs were detectable by Western blots (data not shown).

FATP1 Is Enriched in the Plasma Membrane Fraction in Response to Insulin

In adipocytes and other insulin-sensitive tissues, the glucose transporter Glut4 is translocated to the plasma membrane in response to insulin. Hence, we wanted to test whether the fatty acid transporters FATP1 and/or -4 also change their intracellular localization in response to insulin. To this end serum-starved 3T3 L1 adipocytes were treated with insulin for 60 min, and membranes were prepared by differential centrifugation. FATP1 in serum-starved adipocytes was found only at very low levels in the plasma membrane fraction. However, FATP1 was robustly increased (a 12-fold increase over control) in adipocyte plasma membranes treated with insulin for 60 min, indicative of a net movement of the transporter to the plasma membrane. FATP1 levels in the low-density and high-density microsomal (LDM and HDM, respectively) fractions and in the nuclei/mitochondria/cytoskeletal pellet were reduced after insulin stimulation, indicating that all of these membrane compartments may potentially contribute to the increased pool in the plasma membrane (Figure 2A). In contrast to FATP1, FATP4 was present in the plasma membrane fraction in the basal state and showed a less pronounced increase (2-fold) in this fraction after insulin stimulation. FATP4 was barely detectable in the LDM and HDM fractions but found at robust levels in the nuclei/mitochondria/cytoskeletal pellet. FATP4 levels decreased in this fraction after insulin treatment, suggesting a movement out of the nuclei/mitochondria/cytoskeletal fraction to the plasma membrane (Figure 2A).

Importantly, in insulin-starved cells, FATP1 is found predominantly in the HDM fraction, and intracellular FATP4 is mostly found in the pellet fraction. After insulin stimulation, the increases in levels of FATP1 and -4 in the plasma membrane are paralleled by reductions of FATP1 in the HDM fraction and FATP4 in the pellet fraction. In contrast, the Glut4 pool translocating to the plasma membrane originates predominantly from the intracellular LDM fraction.

Next we wanted to confirm the observed translocation of FATP1 in primary adipocytes. To this end we isolated adipocytes from adult mouse epididymal fat pads. The isolated adipocytes were resuspended in serum free

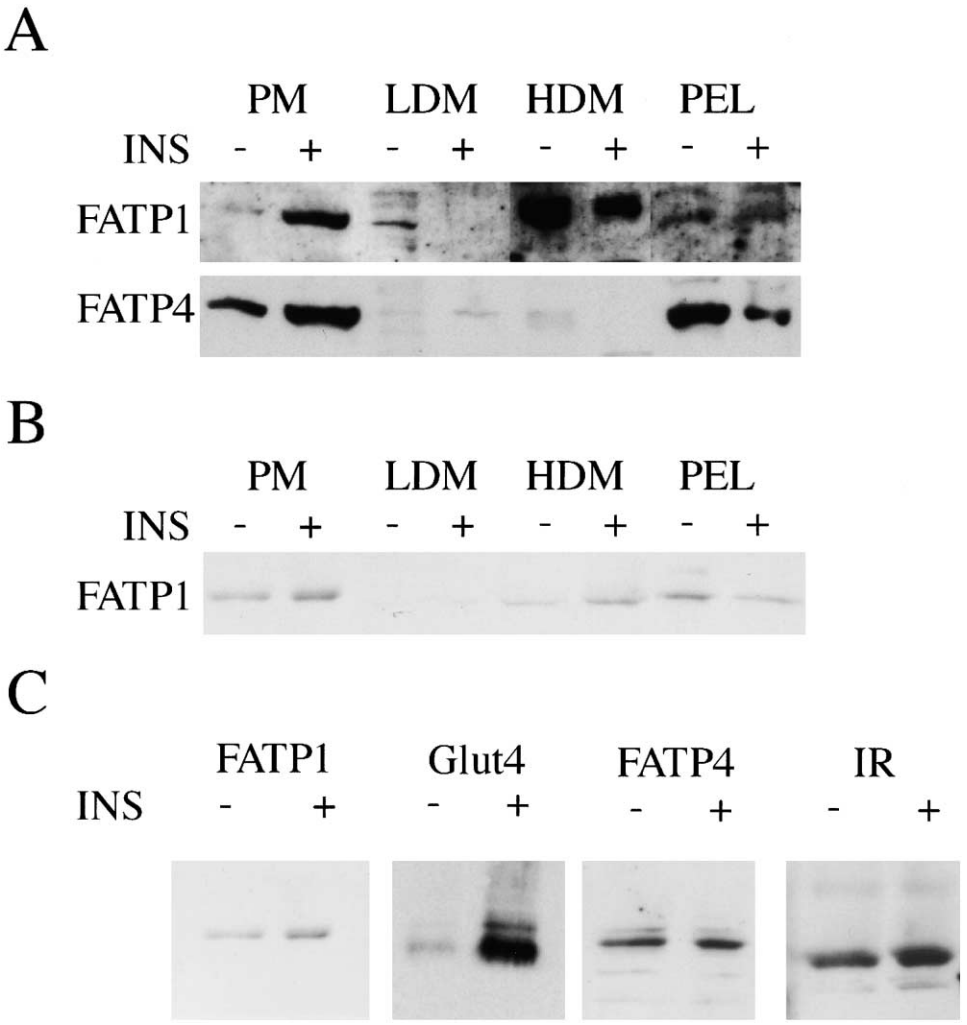

Figure 2. FATP Western Blot of Adipocyte Membrane Fractions

Membrane fractions were prepared by differential centrifugation, and equal amounts of protein were loaded per lane, blotted, and probed with the indicated antibodies. PM, plasma membrane; LDM, low-density membrane; HDM, high-density membrane; PEL, pellet.

(A) Membrane fractions from 3T3 L1 cells serum-starved (−) or treated for 60 min with 50 ng/ml insulin (+) were probed with FATP1- and FATP4-specific anti-sera.

(B) Membrane fractions from primary epididymal adipocytes, which were placed in tissue culture for 30 min with (+) or without (−) insulin (50 ng/ml), were subsequently probed with FATP1-specific antibody.

(C) Plasma membrane fractions from primary epididymal adipocytes, which were placed in tissue culture for 30 min with (+) or without (−) insulin (50 ng/ml), were subsequently probed with either FATP1-, Glut4-, FATP4-, or insulin receptor (IR)-specific anti-sera.

DMEM with or without insulin for 30 min. Membrane fractions were then prepared as were 3T3 L1 cells and probed with the FATP1-specific antibody (Figure 2B). FATP1 was detected in the plasma membrane fraction in the basal and insulin-stimulated states. However, after a 30 min incubation with insulin in tissue culture, the amount of FATP1 in the plasma membrane fraction increased 2-fold. FATP1 levels in the LDM and HDM fraction were low. FATP1 could be found in the nuclei/mitochondria/cytoskeletal fraction in the basal state but was greatly reduced after insulin treatment (Figure 2B), indicating an insulin-triggered movement of FATP1 from this fraction to the plasma membrane.

In order to compare the plasma membrane translocation of FATP1 to other membrane proteins in primary adipocytes, we prepared plasma membranes from 30 min insulin-treated and untreated adipocytes. Equal amounts of total protein were loaded and probed for either FATP1, Glut4, FATP4, or insulin receptor (Figure 2C). Again, a robust (2-fold) increase in FATP1 was observed following insulin treatment. Glut4, which served as a positive control, showed a strong enrichment (4.3-fold) in the plasma membrane fraction, while the insulin receptor, used as a negative control, did not change its localization in the same cells (Figure 2C). Although we could detect FATP4 expression in primary adipocytes, no change in plasma membrane localization was detected in response to insulin (Figure 2C), which contrasts the slight insulin response in 3T3 L1 adipocytes (Figure 2A).

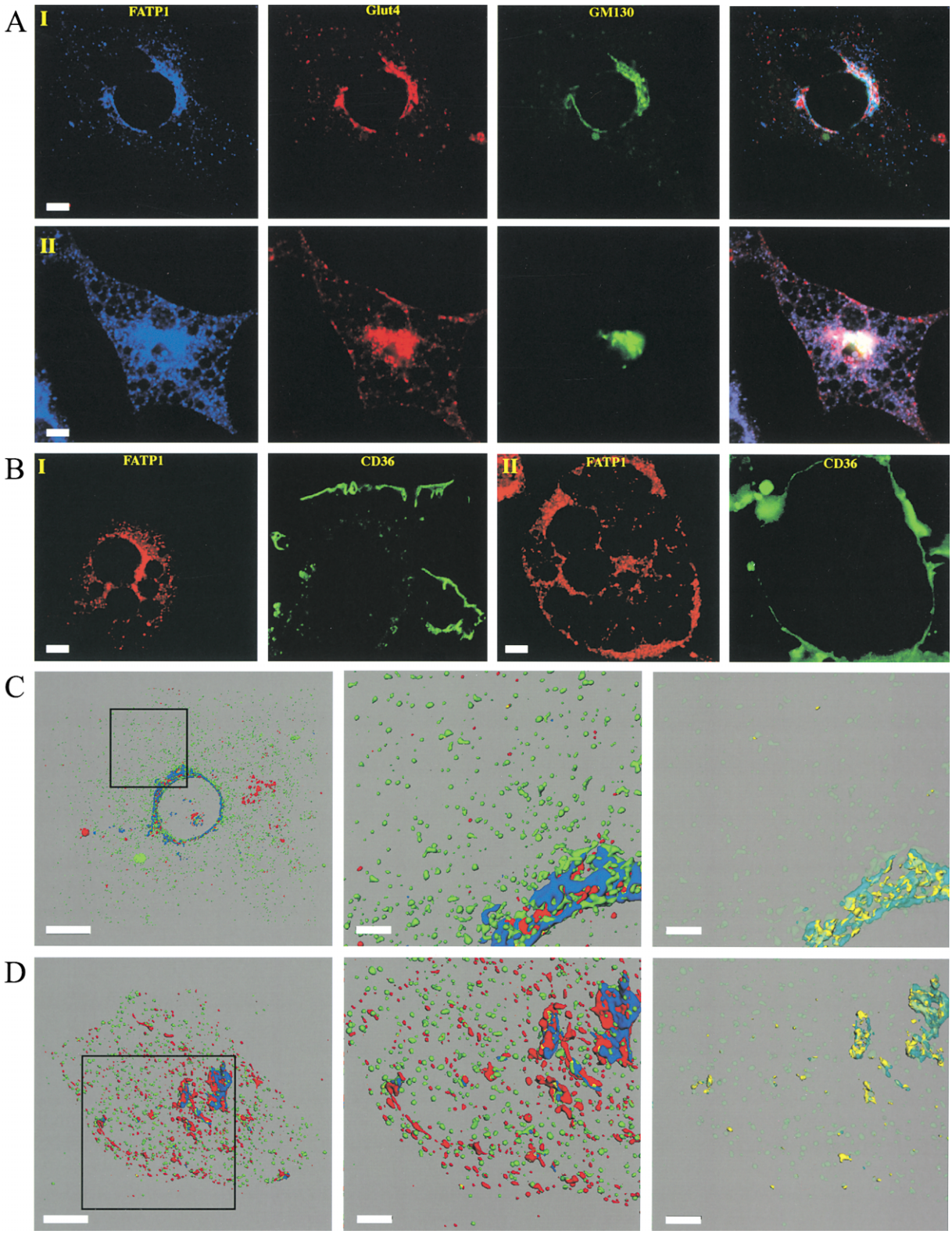

Figure 3. FATP1 Localization by Confocal Immunofluorescence Microscopy

A single z section of a confocal image stack is shown for each channel, as well as the superimposition of all channels (last panel). Bars are 6 μm.

(A) Serum-starved (I) adipocytes or cells treated for 1 hr with 50 ng/ml insulin (II) were costained with antibodies for FATP1, Glut4, and GM130.

(B) Serum-starved (I) adipocytes or cells treated for 1 hr with 50 ng/ml insulin (II) were costained with antibodies for FATP1 and CD36. A single z section of a confocal image stack is shown for each channel.

Insulin Triggers FATP1 Translocation from a Perinuclear Compartment to the Plasma Membrane

To study in further detail the change in subcellular localization of FATPs in adipocytes, we used confocal fluorescent microscopy. Serum-starved or insulin-treated 3T3 L1 adipocytes were stained for FATP1 or -4 and costained with Glut4 and the Golgi-resident protein GM130. Although the FATP4-specific serum showed clear expression of the transporter in enterocytes and other tissues, FATP4 could not be detected in adipocytes by immunofluorescence (data not shown). In serum-starved adipocytes both FATP1 and Glut4 localized to a perinuclear compartment, where both proteins greatly overlapped with the Golgi marker GM130 (Figure 3A [I]). No or little FATP1 was detected on the plasma membrane of these cells, confirming the results from membrane isolation.

Cells treated for 1 hr with insulin showed a distinctively different staining pattern for FATP1 and Glut4 but not for GM130 when compared to the serum-starved cells. Again confirming our membrane fractionation data, we found, after insulin treatment, significant amounts of both FATP1 and Glut4 on the plasma membrane of cells (Figure 3A [II]), indicative of an insulin-regulated exocytosis pathway for both proteins. Additionally, in insulin-treated cells, FATP1 and Glut4 were found in the perinuclear compartment and also in numerous vesicles inside the cytoplasm as well as in close proximity to the plasma membrane. However, no significant colocalization of FATP1 and Glut4 in these vesicles could be detected (Figure 3A [II]).

Next we wanted to compare the subcellular localization of FATP1 to CD36, another protein implicated in fatty acid uptake. Confocal microscopy of serum-starved 3T3 L1 adipocytes revealed that CD36 was located almost exclusively to the plasma membrane, while FATP1 localized predominantly to the perinuclear compartment of the same cell (Figure 3B [I]). FATP1-specific antibodies stained the plasma membrane as well as a multitude of small vesicles throughout the cytoplasm of 3T3 L1 adipocytes treated for 1 hr with insulin, again illustrating the relocalization of the transporter (Figure 3B [II]). In contrast, subcellular localization of CD36 in insulin-treated 3T3 L1 adipocytes was unchanged, with over 90% on the plasma membrane (Figure 3B [I and II]). In insulin-treated, but not in untreated, adipocytes, we observed a partial colocalization of FATP1 and CD36 on the plasma membrane (data not shown).

Since both FATP1 and Glut4 resided in a perinuclear compartment in serum-starved cells and moved to the plasma membrane in response to insulin, we wanted to test the extent of their colocalization in these different subcellular compartments. To achieve sufficiently high-resolution images of small subcellular structures, we acquired 3D confocal image stacks of 3T3 L1 adipocytes and enhanced them by applying deconvolution algorithms. Colocalization of FATP1 with Glut4 was restricted to a perinuclear compartment identified by the Golgi marker GM130. In serum-starved 3T3 L1 adipocytes, both FATP1 and Glut4 colocalized in the perinuclear compartment immunoreactive for GM130 (Figure 3C). After stimulation with insulin, both FATP1 and Glut4 showed increased cytoplasmic distributions. The mean diameters of these cytoplasmic vesicles were similar, 296.54 ± 102.73 nm and 338.49 ± 114.21 nm for FATP1 and Glut4, respectively. Despite this, few peripheral vesicles were immunoreactive for both FATP1 and Glut4 (Figure 3D), suggesting that two different classes of intracellular compartments are used for insulin-triggered exocytosis. This is consistent with results of our subcellular fraction experiments, where, in the absence of insulin, Glut4, FATP1, and FATP2 predominantly reside in different membrane fractions (Figure 2).

Insulin Enhances the Uptake of LCFA into Adipocytes

To study whether the insulin-induced translocation of FATPs correlates with a change in LCFA uptake, we measured the uptake of radiolabeled and fluorescent-labeled LCFAs into adipocytes.

Uptake of [^{14}C]oleate into 3T3 L1 adipocytes was linear over the first five minutes at a final concentration of 50 μM. Initial uptake rates were calculated from linear regression. The oleate uptake rate in serum-starved adipocytes was 3025 pmol/min and nearly doubled to 5280 pmol/min after a 60 min insulin incubation (Figure 4A).

Next we confirmed these results by using albumin-bound C1-BODIPY-C12 fatty acids. C1-BODIPY-C12 FA is a fluorescent LCFA analog that has been well established as a tool for measuring FA uptake in a variety of cell types. In initial experiments we incubated cells for varying amounts of time with C1-BODIPY-C12 FA and used fluorescent-activated cell scanning (FACS) to quantify initial rates of FA uptake of 3T3 L1 adipocytes. We found that incorporation was linear over 5 min (data not shown), and all subsequent experiments were done with 2 min C1-BODIPY-C12 FA incubations. Positive cells were quantitated by determining the percentage of cells above the arbitrary fluorescence cutoff of 20 units in the FL-1 channel (Figure 4B). Comparison of the C1-BODIPY-C12 FA uptake of serum-starved versus

Confocal image stacks were deconvolved and analyzed for 3D colocalization of FATP1 with either the Golgi marker GM130 or Glut4 in 3T3 L1 adipocytes during serum starvation or after insulin stimulation. Fluorescence was isosurface rendered using Imaris3 Surpass. The left panels in (C) and (D) show the entire cell, where the bars represent 7 μm and 3 μm, respectively. In the middle and right panels, the same subregion (boxed) of each cell is shown (bars represent 1.5 μm).

(C) In serum-starved 3T3 L1 adipocytes, both FATP1 (green) and Glut4 (red) are predominantly localized (left and middle panels) to the perinuclear region containing GM130 (blue). In the second panel the colocalization between FATP1 and Glut4 (yellow) and between FATP1 and GM130 (turquoise) is shown. Both colocalized signals are restricted to the perinuclear region.

(D) After insulin stimulation, an increased number of vesicles containing FATP1 and Glut4 are present within the cytoplasm and at the plasma membrane (left and middle panels). Colocalization between both FATP1 and Glut4 (yellow) and FATP1 and GM130 (blue) remains predominantly limited to the perinuclear region, with few vesicles containing both FATP1 and Glut4.

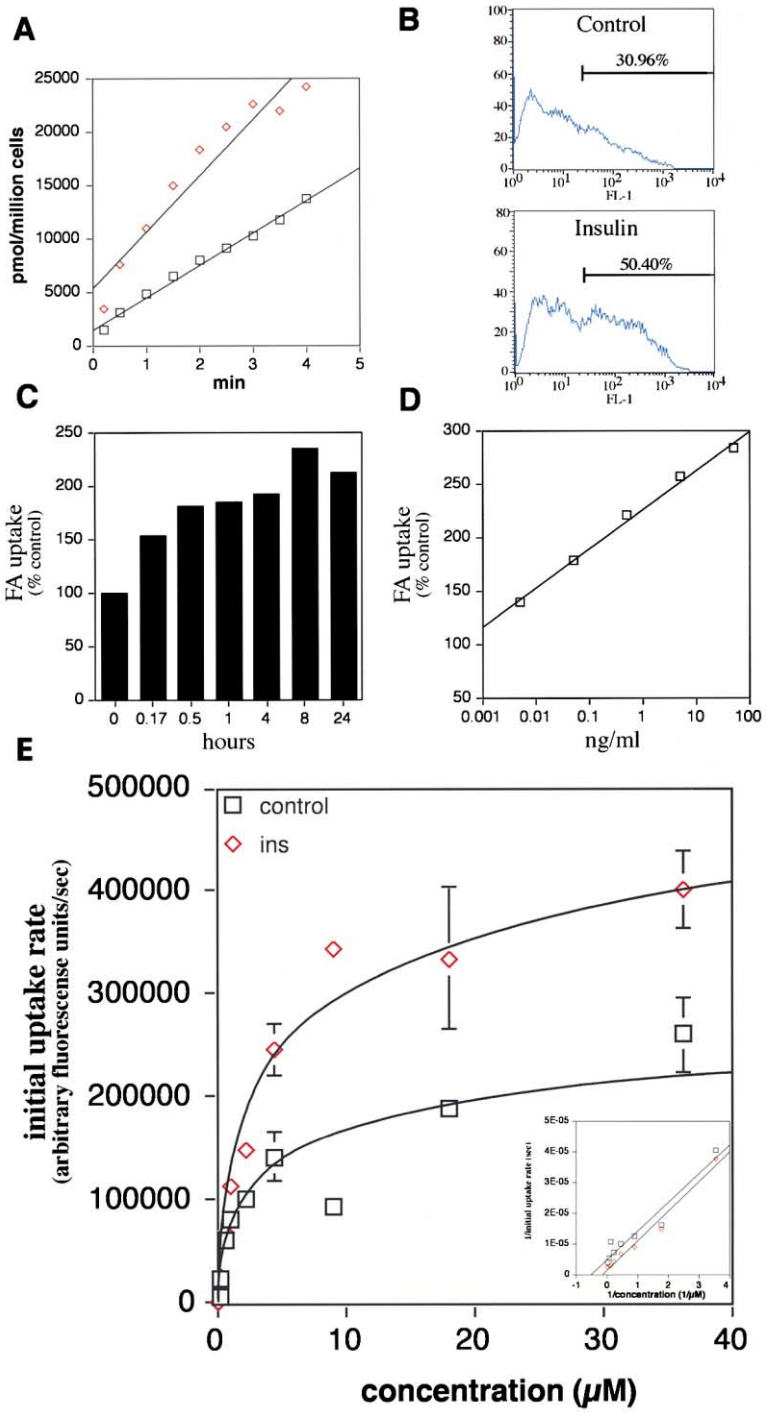

Figure 4. Effect of Insulin on LCFA Uptake into Adipocytes

(A) Uptake of [^{14}C]oleate (50 μM) into serum-starved (squares) or insulin-treated (diamonds) 3T3 L1 adipocytes was measured over 4 min. Lines indicate curve fits based on linear regression, yielding uptake constants of 3025 pmol/min (squares) and 5280 pmol/min (diamonds) per million cells, respectively.

(B) Two minute uptake of C1-BODIPY-C12 FA into 3T3 L1 adipocytes serum starved (control) or treated for 1 hr with 50 ng/ml insulin (insulin) was quantitated by FACS. Bars indicate the arbitrary gate used to define positive cells.

(C) C1-BODIPY-C12 FA uptake assays as shown in (B) were used to determine the effect of 50 ng/ml insulin over time. Values for the percentage of positive insulin-treated cells were matched for each time point to the percentage of positive control cells in serum-free medium.

(D) C1-BODIPY-C12 FA uptake assays as shown in (B) were used to determine the effect of the indicated concentration of insulin on LCFA uptake after an 8 hr incubation. Note the logarithmic scale for the insulin concentration.

(E) Initial rates of uptake (30 s) of *cis*-parinaric acid were determined for 3T3 L1 adipocytes, which were either serum starved (squares) or treated with 50 ng/ml insulin for 8 hr (diamonds). A double reciprocal plot of the data (Lineweaver-Burk diagram shown in insert) was used to determine K_m and V_{max} for control cells (squares; 160 mmol/s, 1.5 μM) and insulin-treated cells (diamonds; 330 mmol/s, 2 μM).

insulin-treated cells showed again a robust enhanced uptake in cells preincubated with insulin (31% versus 50% after 30 min of insulin) (Figure 4B).

A time course of insulin's effect on C1-BODIPY-C12 FA showed that uptake was enhanced within 15 min (153% of control), reached a plateau over the next 4 hr, with an average increase of 185% compared to cells in serum-free medium for the same amount of time, and increased slightly further after 8–24 hr, with an average long-term insulin effect of 225% of control (Figure 4C).

Insulin titration with an incubation time of 8 hr showed a logarithmic dose response with a significant increase of C1-BODIPY-C12 uptake (140% over control), detectable even at the lowest insulin concentration tested (0.005 ng/ml insulin), and half-maximal stimulation around 1 ng/ml (Figure 4D).

As a third method of characterizing insulin's effect on LCFA uptake by adipocytes, we used the naturally occurring LCFA *cis*-parinaric acid. Varying the concentration of *cis*-parinaric acid showed that initial uptake

Table 1. Regulation of LCFA Uptake

Preincubation	Treatment	LCFA Uptake (% Control)
Ten minutes	insulin	181
Thirty minutes plus ten minutes	wortmanin plus insulin	119
Thirty minutes plus ten minutes	PD98059 plus insulin	95
Sixteen hours plus ten minutes	TNF-α plus insulin	60
Ten minutes	Englitazone	95
Sixteen hours	Englitazone	185
Ten minutes	murine TNF-α	41
Ten minutes	human TNF-α	50
Ten minutes	sphingomyelinase	29
Ten minutes	ceramide	32
Ten minutes	glucagon	14
Ten minutes	forskolin	7
Ten minutes	isoproterenol	12
Ten minutes	AlF4	25
Ten minutes	8-Br-cAMP	33

velocities of this LCFA into both serum-starved and insulin-treated (16 hr incubation) adipocytes were saturable (Figure 4E). Lineweaver-Burk diagrams of the reciprocal uptake velocities versus reciprocal concentration for both serum-starved and insulin-treated adipocytes could be fitted to a linear equation with simple Michaelis-Menten kinetics (Figure 4E, insert). Linear equations from these plots were used to calculate the apparent K_m and V_{max} for control and insulin-treated cells. Importantly, insulin treatment (16 hr incubation) more than doubled the V_{max} for *cis*-parinaric acid uptake into adipocytes, from 160 mmol/s to 330 mmol/s, while, at the same time, the apparent K_m for uptake of this LCFA remained virtually constant (1.5 μM versus 2 μM) (Figure 4E). These observations are consistent with an increase in active LCFA transporters on the cell surface, further supporting our hypothesis that FATP translocation to the plasma membrane is responsible for enhanced LCFA uptake after insulin stimulation.

Next we performed a preliminary pharmacological characterization of the insulin-signaling pathway, leading to increased uptake of LCFAs. Table 1 shows that insulin stimulation of LCFA uptake was partially inhibited by both PI3 kinase inhibitors (wortmannin) as well as MAP kinase (MEK) inhibitors (PD98059), suggesting that at least two different signaling cascades emanating from the receptor are involved in this insulin effect (Table 1). Since antidiabetic thiazolidinediones such as englitazone have been shown to lower blood glucose as well as LCFA levels, we wanted to test englitazone's effect on LCFA uptake into 3T3 L1 adipocytes. In line with its function as a transcriptional activator, we found that englitazone indeed stimulates LCFA uptake into adipocytes after 16 hr incubation but not after a short-term (10 min) treatment (Table 1).

Insulin Effect on Downstream Metabolic Reactions

Since insulin could potentially change LCFA uptake not only by modifying transport but also by changing subsequent steps that may effect intracellular LCFA pools, we investigated insulin's effect on lipolysis, LCFA efflux, and β oxidation in 3T3 L1 cells. Intracellular lipases such as hormone-sensitive lipase generate fatty acids and glycerol from triglycerides. The intracellular glycerol quickly equilibrates with the extracellular medium so that hormone-sensitive lipase activity can be assessed by measuring extracellular glycerol concentrations. To this end, serum-starved 3T3 L1 adipocytes were incubated either 30 min or overnight with insulin, TNF-α, or isoproterenol, and glycerol efflux was measured over 30 min. Glycerol accumulation in the medium was linear over this period of time, and linear regression was used to assess efflux rates. After 30 min treatments with isoproterenol, a known activator of hormone-sensitive lipase, we observed a robust increase in glycerol efflux (1.5 μg/min for control versus 12.2 μg/min for isoproterenol), while insulin had no effect (1.8 μg/min), and TNF-α cased a slight increase (2.8 μg/ml) (Figure 5A). Similarly, changes in glycerol efflux caused by insulin (1.4 μg/ml) and TNF-α (2.8 μg/ml) after 16 hr treatment were insignificant compared to the twenty-fold increase in glycerol efflux rates caused by isoproterenol (1.3 μg/ml for control versus 22.2 μg/ml for isoproterenol) (Figure 5A). Further, insulin was able to stimulate LCFA uptake independently of increased glucose uptake, as a 15 min insulin stimulation of adipocytes in glucose-free medium led to a 64% increase of [^{14}C]oleate uptake (data not shown). Longer incubation (1 hr) in glucose-free medium greatly diminished both basal and insulin-stimulated LCFA uptake.

To confirm these indirect measurements of lipase activity, we incubated adipocytes with [^{14}C]oleate overnight and measured efflux of radioactivity after 1 hr treatment with insulin, TNF-α, isoproterenol, or forskolin. [^{14}C]oleate efflux was unchanged by insulin and TNF-α but elevated by isoproterenol and forskolin (Figure 5B), confirming the results obtained from glycerol measurements.

One further explanation for the insulin-mediated increase in LCFA uptake is depletion of intracellular LCFA pools through increased oxidation. However, we found that, after measuring the β oxidation rates of 3T3 L1 adipocytes, a 1 hr incubation with insulin significantly lowered, and not increased, LCFA oxidation rates (116 ± 1.6 pmol/hr for versus 33 ± 3.1 pmol/hr for insulin). TNF-α had no effect (118 ± 15.7 pmol/hr) after 1 hr. Further, β oxidation rates after 16 hr incubations with either insulin (160 ± 5 pmol/hr) or TNF-α (146 ± 38 pmol/hr) were not significantly different than those for control

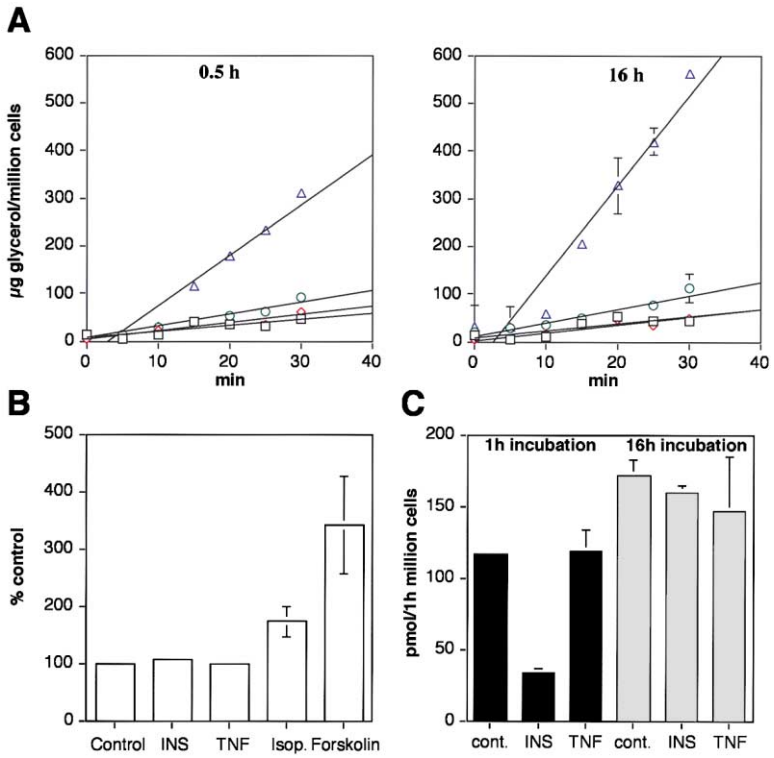

Figure 5. Effect of Insulin on LCFA Efflux and β Oxidation

(A) 3T3 L1 adipocytes in 12 well plates were treated for 30 min or 16 hr with 50 ng/ml insulin (diamonds), 50 ng/ml TNF-α (circles), or 10 μM isoproterenol (triangles). Cumulative glycerol concentrations were measured over 30 min, after which the cells were detached and counted. Glycerol concentrations were normalized to cell numbers, and triplicate measurements were plotted over time. Lines represent linear regressions through the data points. The release constants per million cells were as follows: control (0.5 hr, 1.5 μg/min and 16 hr, 1.3 μg/min); insulin (0.5 hr, 1.8 μg/min and 16 hr, 1.4 μg/min); TNF-α (0.5 hr, 2.8 μg/min and 16 hr, 2.8 μg/min); isoproterenol (0.5 hr, 12.2 μg/min and 16 hr, 22.2 μg/min).

(B) 3T3 L1 adipocytes were incubated overnight with 50 μM [^{14}C]oleate and washed, and efflux of radioactivity was determined over 30 min in serum-free medium (control), 50 ng/ml insulin, 50 ng/ml TNF-α, 10 μM isoproterenol, or 10 μM forskolin. Efflux was determined for each well by expressing the ratios of activity in the supernatant to the total activity found in the supernatant and the cells. All measurements were done in quadruplicate.

(C) β oxidation assays with 3T3 L1 adipocytes were performed as described in the experimental procedure section. Adipocytes were incubated for either 1 hr or 16 hr with insulin (INS), TNF-α (TNF), or in a serum-free medium (cont.). Experiments were done in triplicates, and oxidation rates per million cells were as follows: control (1 hr, 116 ± 2 pmol/hr and 16 hr, 171 ± 11 pmol/hr); insulin (1 hr, 33 ± 3 pmol/hr and 16 hr, 160 ± 5 pmol/hr); TNF-α (1 hr, 118 ± 16 pmol/hr and 16 hr, 146 ± 38 pmol/hr).

cells (171 ± 11 pmol/hr) (Figure 5C), while LCFA uptake was clearly increased (Figure 1).

TNF-α Suppresses LCFA Uptake and FATP Protein Expression

TNF-α is known to antagonize many of insulin's effects on cells and to cause insulin desensitization in adipocytes and muscle cells. A 16 hr treatment of 3T3 L1 adipocytes with TNF-α led to a 50% reduction in the uptake rate of [^{14}C]oleate compared to serum-starved adipocytes (3025 pmol/min for control versus 1421 pmol/min for TNF-α) (Figure 6A). An agonistic antibody against the 55 kDa TNF-α receptor showed a similar effect (1436 pmol/min) (Figure 6A), indicating that the 55 kDa TNF-α receptor is sufficient for signaling.

As with insulin, we further analyzed this effect using the LCFA analog C1-BODIPY-C12. A 1 hr TNF-α treatment inhibited the uptake of C1-BODIPY-C12 FA by 46% (Figure 6B). A time course of the TNF-α effect on C1-BODIPY-C12 FA uptake showed a clear biphasic mode of action. A fast response, which is observed after minutes, inhibits 50% of C1-BODIPY-C12 FA uptake into adipocytes followed by a second response, observed after 8–24 hr of TNF-α incubation, suppressing C1-BODIPY-C12 FA uptake by up to 90% (Figure 6C). TNF-α pretreatment followed by a 10 min insulin stimulus showed that not only basal but also insulin-stimulated LCFA uptake were blocked by this cytokine (Table 1).

The hypothesis that the TNF effect is mainly mediated by the 55 kDa TNFR was further supported by the fact that human TNF-α, which can only bind to the 55 kDa receptor on murine cells, had a similar effect to mouse TNF-α (Table 1) and by our finding that two molecules, sphingomyelinase and ceramide, which have been implicated in 55 kDa TNFR signaling, also strongly inhibited LCFA uptake within minutes (Table 1).

As shown in the previous section, TNF-α had no significant effect on lipoprotein lipase activity (Figure 5A), LCFA efflux (Figure 5B), or β oxidation (Figure 5C), so it seems likely that the short-term effect (15 min–4 hr) is primarily due to inhibition of basal insulin signaling. To explain the significant further reduction in LCFA uptake after 8–24 hr, we tested the effects of TNF-α and TNFR agonist antibodies on FATP expression. Both TNF-α and the antibody caused a significant reduction (60% inhibition) of FATP1 and -4 protein expression as assessed by Western blots (Figure 6D). Interestingly, in the same experiment, 16 hr incubation of adipocytes with insulin caused only a modest (FATP1) or no (FATP4) increase in FATP expression, suggesting that insulin acts mainly by changing FATP subcellular localization while TNF-α both inhibits insulin signaling and additionally reduces LCFA uptake by suppressing FATP transcription.

Discussion

Upon insulin stimulation both FATP1 and Glut4 were found on the adipocyte plasma membrane, in numerous small vesicles, and in a perinuclear compartment. The peripheral FATP-containing vesicle populations showed only marginal overlap with Glut4-containing vesicles.

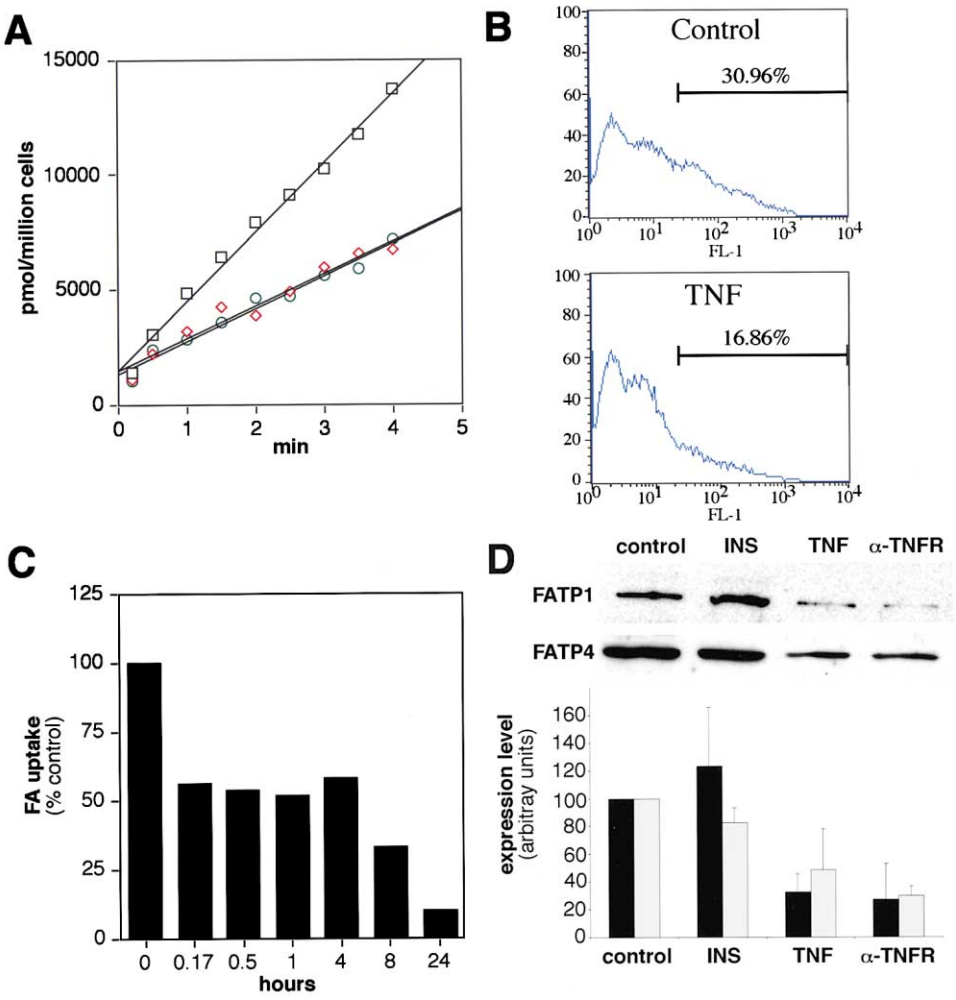

Figure 6. Effect of TNF-α on LCFA Uptake and FATP Expression in 3T3 L1 Adipocytes

(A) Uptake of [^{14}C] oleate (50μM) into serum-starved (squares), TNF-α-treated (diamonds), or anti-TNFR-treated (circles) 3T3 L1 adipocytes (all in the absence of serum) was measured over 4 min. Lines indicate curve fits based on linear regression, yielding uptake constants of 3025 pmol/min (squares), 1421 pmol/min (diamonds), and 1436 pmol/min (circles) per million cells, respectively.

(B) Two minute uptake of C1-BODIPY-C12 FA into 3T3 L1 adipocytes serum starved (control) or treated for 1 hr with 50 ng/ml TNF-α in the absence of serum (TNF) was quantitated by FACS. Bars indicate the arbitrary gate used to define positive cells.

(C) C1-BODIPY-C12 FA uptake assays as shown in (B) were used to determine the effect of 50 ng/ml TNF-α over time. Values were matched for each time point to control cells in serum-free medium.

(D) 3T3 L1 adipocytes were either treated with insulin, TNF-α, or anti-TNFR antibody, lysed, adjusted for equal protein concentration, and probed in Western blots for FATP1 and -4 expression. Bands for FATP1 (black bars) and FATP4 (gray bars) were quantitated by densitometry and normalized to the controls. An average of three independent experiments is shown.

While 3D image analysis showed that the average vesicle diameters were similar, only 3.37% of FATP1 immunoreactivity coincided with that of Glut4. This suggests that insulin-triggered plasma membrane targeting of glucose and fatty acid transporters occurs via two independent vesicular pathways.

Membrane fractionation data confirmed that the insulin regulated exocytosis pathway of FATP1 differs from the well-characterized Glut4 pathway. Although both FATP1 and Glut4 are increased on the plasma membrane in response to insulin, they differ in the compartments from which they originate. It has been repeatedly demonstrated that the initially translocated Glut4 is derived from a dispersed vesicular storage compartment and early endosomes (Holman and Sandoval, 2001), and both fractionate in the light microsomal (LDM) fraction. In contrast, FATP1 is predominantly found in the HDM and pellet fractions. After insulin stimulation FATP1 is reduced in all but the plasma membrane fractions. Importantly, the most notable contribution to the increased plasma membrane pool is derived from the HDM, and not from the LDM, fraction. It remains to be determined whether these divergences are attributable to differences in FATP1 recycling and trafficking through the endosomal compartment, strong interactions of the FATP1 exocytic vesicles with the cytoskeleton, or other causes.

Blocking PI3 kinase activation with wortmannin inhibits insulin-triggered translocation of both FATP1 (this paper) and Glut4 to the cell surface (Cheatham, 2000;

Holman and Sandoval, 2001) as well as insulin-stimulated LCFA uptake. In contrast, inhibiting the MAP kinase cascade with the MEK inhibitor PD98059 does not affect Glut4 translocation (Kayali, et al., 2000; Fujishiro, et al., 2001), while we show here that insulin-induced FATP1 translocation is significantly reduced. Thus, different signal transduction pathways downstream of the insulin receptor are required for Glut4 and FATP1 translocation, consistent with the notion that these proteins are localized in different intracellular compartments prior to fusion with the plasma membrane. Clearly, further studies are needed to confirm these points and to compare the dynamics of FATP1 and Glut4 trafficking.

It also remains to be determined whether FATP translocation is sufficient for activation of LCFA uptake or whether the transporter has to be additionally modified or requires cooperative interaction with other proteins. One other protein implicated in LCFA uptake into adipocytes and other tissues is the scavenger receptor CD36/FAT (Abumrad et al., 1993). Interestingly, Bonen et al. reported that contractile activity in skeletal muscle increased CD36 expression (Bonen et al., 1999) and stimulated translocation of CD36 from an intracellular compartment to the plasma membrane (Bonen et al., 2000). However, using a mouse monoclonal anti-CD36 serum (Febbraio et al., 2000), we were unable to detect significant intracellular pools of CD36 either in serum-starved or insulin-stimulated adipocytes. This does not exclude the possibility that an FATP/CD36 interaction on the plasma membrane is required for efficient LCFA uptake (Abumrad et al., 2000; Stahl et al., 2001).

Insulin-induced FATP translocation in adipocytes was paralleled by enhanced uptake of LCFAs. A doubling of LCFA uptake rates in response to insulin was confirmed by three different assays based on the uptake of [^{14}C]oleate, C1-Bodipy-C12, and *cis*-parinaric acid. *Cis*-parinaric uptake assays, which allow for an exact determination of the free fatty acid concentration (Fraser et al., 1997), showed that the increased uptake was mainly due to an increase in initial uptake velocities (160 mmol/s versus 330 mmol/s) while the K_m remained relatively unchanged (1.5 μM versus 2 μM). This is indicative of a quantitative, rather than qualitative, difference in uptake, suggesting that more FATPs were present on the plasma membrane after insulin stimulation. Insulin-induced increases in LCFA uptake were partially blocked by inhibitors of MAP kinase and PI3 kinase, implicating both signaling pathways in the signaling cascade emanating from the insulin receptor and resulting in enhanced LCFA uptake.

Insulin changes a multitude of cellular responses, including inhibition of lipolysis (Holm et al., 2000), raising the possibility that increased LCFA uptake is primarily due to secondary effects on adipocyte metabolism. This may result in a lowered intracellular LCFA concentration and, hence, increased LCFA influx. Catecholamines induce lipolysis by elevating cAMP levels, leading to the activation of hormone-sensitive lipase. This process can be counteracted by insulin through activation of phosphodiesterase 3B, which decreases cAMP levels. However, the experiments presented here were mainly done using serum-starved cells showing a very low basal hormone-sensitive lipase activity that was not further suppressed by insulin. Insulin also increased LCFA uptake in the absence of glucose, indicating that the effect was not secondary to increased glucose uptake and 3-phosphoglycerate production. Also, β oxidation was not increased, but rather suppressed, by insulin. Although we cannot conclude from these observations that the insulin-mediated increase in LCFA uptake is solely due to increased transport across the plasma membrane, it is very likely that the increased number of FATPs on the cell surface have a significant and, perhaps, rate limiting contribution to LCFA uptake by adipocytes.

A positive link between FATP protein levels and fatty acid uptake has been established by overexpressing FATP1 and other family members, resulting in increased LCFA uptake (Hirsch et al., 1998; Schaffer and Lodish, 1994; Stahl et al., 1999). Despite a doubling of LCFA uptake and FATP1 translocation during a 16 hr insulin treatment of 3T3 L1 adipocytes, total FATP1 and -4 total protein levels remained unchanged, supporting the hypothesis that a posttranslational event is responsible for enhanced LCFA uptake. Our observation that insulin does not significantly change FATP1 protein levels is in contrast to the finding that insulin reportedly downregulated FATP1 mRNA levels within hours (Man et al., 1996).

We established a further link between FATP expression and fatty acid uptake into adipocytes by demonstrating that a 16 hr treatment with TNF-α reduces FATP1 and -4 protein levels by 60% and, at the same time, inhibits basal and insulin-stimulated uptake by 80% and 67%, respectively. TNF-α only marginally affected lipolysis and had no effect on β oxidation or LCFA efflux. Interestingly, LPS and TNF-α have also been reported to reduce FATP1 levels in liver and adipose tissue of Syrian hamsters (Memon et al., 1998).

TNF-α is known to impact glucose utilization of tissues by a dual action, inhibition of insulin signaling and transcriptional repression of proteins involved in glucose uptake, most notably that of Glut4 (Hotamisligil, 2000). Interestingly, the time course of TNF-α-mediated inhibition of LCFA uptake is biphasic, showing an inhibition of approximately 50% at early time points and further inhibition up to 80% after 8–16 hr. Similarly, a dual effect of TNF-α is seen on LCFA uptake; a fast inhibition of insulin signaling, possibly through phosphorylation of IRS-1 (Hotamisligil et al., 1996), and an additional delayed effect through the inhibition of FATP expression. TNF-α can bind 55 and 75 kDa receptors on murine cells. The 55 kDa receptor is sufficient to mediate TNF-α signaling, leading to insulin desensitization and Glut4 downregulation (Hube and Hauner, 2000). Inhibition of insulin signaling through stimulation of the p55 TNF receptor is coupled to the activation of sphingomyelinase (Peraldi et al., 1996). The 55 kDa receptor was also sufficient to mediate TNF-α inhibition of LCFA uptake, demonstrated using an agonist antibody specific for the 55 kDa receptor (Tartaglia et al., 1993) and human TNF-α, which only binds the 55 kDa murine receptor and was as efficient as murine TNF-α. Both exogenous sphingomyelinase as well as ceramide inhibited LCFA uptake, indicating further similarities between the TNF signaling pathways involved in the inhibition of glucose and LCFA uptake.

In conclusion, we have demonstrated that uptake of LCFAs into adipocytes is a regulated process sharing

many similarities with hormone regulated glucose uptake. We propose that this regulation is mainly due to translocation of FATP1 to the plasma membrane and is further controlled by transcriptional regulation of FATPs. It is interesting to note that both Glut4 and FATP1 and -4 proteins are also coexpressed in other insulin-sensitive tissues, such as skeletal muscle and heart (Stahl et al., 2001). Thus, we hope that these observations will improve our knowledge of the molecular mechanisms underlying insulin-regulated LCFA uptake into many hormone-sensitive tissues and further our understanding of normal energy homeostasis and metabolic disorders such as type 2 diabetes.

Experimental Procedures

Materials

BODIPY FA (C1-BODIPY-C12) was obtained from Molecular Probes, [^{14}C] oleate was purchased from ARC, TOTO-3 was purchased from Molecular Probes, and all other materials were obtained from Sigma.

Antibodies

Polyclonal anti-sera against the C termini of FATP1 and -4 were raised as described (Stahl et al., 1999), and mouse anti-GM130 was purchased from Signal Transduction Labs. Glut4-specific antibodies were from Santa Cruz Biotechnology, and the mouse monoclonal anti-CD36/FAT antibody was a generous gift from Dr. Maria Febbraio.

Preparation of Primary Mouse Adipocytes

Visceral fat pads were removed from groups of male and female Balb-C mice after the animals were sacrificed. Fat pads were cut into ~1 cm^3 pieces with scissors in Krebs Ringer buffer (KRB) and resuspended in KRB solution containing 3 mg/ml type 1 collagenase (Worthington). Cells were incubated for 1 hr with gentle shaking and washed three times with KRB containing 2% BSA and twice with DMEM.

Fluorescent FA and [^{14}C]oleate Uptake Assay

LCFA uptake with fluorescent and radioactive fatty acids was assayed as previously described (Hirsch et al., 1998).

Efflux Essays

Day 8 3T3 L1 adipocytes were trypsinized and seeded into 48 well plates. Cells were incubated overnight with tissue culture medium containing 0.1% BSA and 50 μM [^{14}C]oleate. Unincorporated FAs were removed by three washes with PBS/0.1% BSA followed by a 30 min incubation of the cells with tissue culture medium containing 0.1% BSA and the indicated hormones at 37°C. Supernatants and cells were removed from the plate and subjected to β scintillation counting. In order to normalize for well to well differences in adipocyte number, efflux was determined for each well by expressing the ratios of radioactivity in the supernatant to the total radioactivity found in the supernatant and the cells. All measurements were done in quadruplicate.

Cis-Parinaric Acid Uptake Assay

Cis-parinaric acid (Molecular Probes) uptake measurements were performed as described (Fraser et al., 1997). Briefly, 3T3 L1 adipocytes were harvested using EDTA and resuspended in mammalian Krebs-Ringer solution at a concentration of 100,000 cells/ml. While the cells were constantly stirred with a magnetic stir bar, *cis*-parinaric acid was added as a 100-fold concentrated stock to yield the indicated final concentrations. After the addition of *cis*-parinaric acid (time point 0), fluorescence intensity at 324 nm was monitored at 0.5 s intervals (Fluorolog, ISA Instruments) over 60 s. Uptake rates over the initial 30 s were determined using linear regression.

Glycerol Efflux Assays

An equal number of adipocytes were placed in six well plates and treated with the indicated substances in a total volume of 2 ml medium. For glycerol measurements 100 μl aliquots of supernatant were taken from each well every 5 min. At the end of the assay, the cells were detached and counted. Glycerol concentration was determined using GPO-Trinder reagent and a glycerol standard (both Sigma Diagnostics) according to the manufacturer's instructions. Based on the total volume in the wells at the time of sample withdrawal, total glycerol content was calculated and normalized to 1 million cells.

Membrane Isolations

After the indicated treatments, four 10 cm plates of 3T3 L1 adipocytes were washed once with cold 250 mM sucrose, 10 mM Tris (pH 7.4), and 0.5 mM EDTA (buffer A). All subsequent steps were performed at 4°C. Cells were resuspended by scraping in cold buffer A with protease inhibitors and then homogenized using 16 strokes in a tight-fitting Dounce-type Teflon tissue grinder. The homogenates were centrifuged at 11,500 rpm in an SS-34 rotor (16,000 × g) for 20 min. The pellet was resuspended in buffer A and then layered on top of 1.12 M sucrose, 10 mM Tris (pH 7.4), and 0.5 mM EDTA in an ~2 ml centrifuge tube. The samples were centrifuged in a TLS-55 rotor at 36,000 rpm (158,000 × g) for 20 min. The pellet from this centrifugation (PEL) was resuspended in RIPA buffer (20 mM Tris, 1% NP-40, 0.5% sodium deoxycholate, and 0.1% sodium dodecyl sulfate [pH 7.8]) after the interface (1 ml) was removed using a syringe, diluted with an additional 1 ml of buffer A, and centrifuged in a TLA-100.2 rotor at 37,000 rpm (74,000 × g) for 9 min. The pellet from this centrifugation, designated PM, was resuspended in RIPA buffer and stored at −20°C until needed. The supernatant from the initial centrifugation was recentrifuged at 19,000 rpm in an SS-34 rotor (43,000 × g) for 30 min. The pellet (designated HDM) was resuspended in RIPA buffer and stored at −20°C. The supernatant was centrifuged at 65,000 rpm in a Ti70.1 rotor (39,000 × g) for 75 min. The pellets from this centrifugation, designated LDM, were resuspended in RIPA buffer and stored at −20°C.

Fluorescence Microscopy, Image Restoration, and Analysis

3T3 L1 adipocytes were transferred onto gelatin-coated glass cover slips and allowed to adhere overnight. Cells were fixed in 2% paraformaldehyde in Hanks buffered salt solution (HBS, Gibco/BRL) and blocked with 2% BSA, 10% FCS, 1% normal donkey serum, and 0.5% saponin in HBS (blocking buffer) for 1 hr. Cells were then incubated with the indicated antibodies in blocking buffer, washed with blocking buffer without donkey serum, and incubated with secondary antibodies conjugated to FITC, CY-3, or Cy-5. After the cells were washed and mounted (SlowFade or Prolong, Molecular Probes), they were visualized using a Zeiss LSM510 laser scanning confocal microscope. Laser lines, pinhole settings, and emission filters were used as appropriate for the maximum signal for each dye. Bleedthrough between separate emission channels was reduced through use of the multitracking feature of the Zeiss LSM510 microscope. For deconvolution, images were collected according to the Nyquist sampling theory for the shortest wavelength of the dyes used. Typically, voxel dimensions were 75 nm × 75 nm × 100 nm (x:y:z). Confocal data were deconvolved using the MLE algorithm within Huygens2 (Scientific Volume Imaging, Amsterdam) on an Origin 2200 (Silicon Graphics, CA). Colocalization software (Bitplane, Zurich) was used for analysis of 3D colocalization between fluorescence channels in restored data. 3D image rendering, object extraction, and volume determination used Imaris 3.1 Surpass (Bitplane, Zurich).

Acknowledgments

The authors thank Dr. Tsu-Shuen Tsao for his expert help in performing the β oxidation assays. We thank Dr. Maria Febbraio for providing the CD36 monoclonal antibody. Part of this work was conducted utilizing the W.M. Keck Foundation Biological Imaging Facility at the Whitehead Institute, and we thank Nicki Watson for her help in using the facility. This work was supported by the NIH grants PO1HL-4148412, 1-PO1-HL66105-01, and RO1-DK47618-13.

Received: October 10, 2001
Revised: March 6, 2002

References

Abumrad, N.A., el-Maghrabi, M.R., Amri, E.Z., Lopez, E., and Grimaldi, P.A. (1993). Cloning of a rat adipocyte membrane protein implicated in binding or transport of long-chain fatty acids that is induced during preadipocyte differentiation. Homology with human CD36. J. Biol. Chem. *268*, 17665–17668.

Abumrad, N.A., Forest, C.C., Regen, D.M., and Sanders, S. (1991). Increase in membrane uptake of long-chain fatty acids early during preadipocyte differentiation. Proc. Natl. Acad. Sci. USA *88*, 6008–6012.

Abumrad, N.A., Sfeir, Z., Connelly, M.A., and Coburn, C. (2000). Lipid transporters: membrane transport systems for cholesterol and fatty acids. Curr. Opin. Clin. Nutr. Metab. Care *3*, 255–262.

Bonen, A., Dyck, D.J., Ibrahimi, A., and Abumrad, N.A. (1999). Muscle contractile activity increases fatty acid metabolism and transport and FAT/CD36. Am. J. Physiol. *276*, E642–649.

Bonen, A., Luiken, J., Arumugam, Y., Glatz, J., and Tandon, N. (2000). Acute regulation of fatty acid uptake involves the cellular redistribution of fatty acid translocase. J. Biol. Chem. *275*, 14501–14508.

Cheatham, B. (2000). GLUT4 and company: SNAREing roles in insulin-regulated glucose uptake. Trends Endocrinol. Metab. *11*, 356–361.

Cherrington, A.D. (1999). Banting lecture 1997. Control of glucose uptake and release by the liver in vivo. Diabetes *48*, 1198–1214.

Coburn, C.T., Hajri, T., Ibrahimi, A., and Abumrad, N.A. (2001). Role of CD36 in membrane transport and utilization of long-chain fatty acids by different tissues. J. Mol. Neurosci. *16*, 117–121; 151–157.

Febbraio, M., Podrez, E.A., Smith, J.D., Hajjar, D.P., Hazen, S.L., Hoff, H.F., Sharma, K., and Silverstein, R.L. (2000). Targeted disruption of the class B scavenger receptor CD36 protects against atherosclerotic lesion development in mice. J. Clin. Invest. *105*, 1049–1056.

Fraser, H., Coles, S.M., Woodford, J.K., Frolov, A.A., Murphy, E.J., Schroeder, F., Bernlohr, D.A., and Grund, V. (1997). Fatty acid uptake in diabetic rat adipocytes. Mol. Cell. Biochem. *167*, 51–60.

Frayn, K.N. (1998). Non-esterified fatty acid metabolism and postprandial lipaemia. Atherosclerosis *141*, S41–46.

Fujishiro, M., Gotoh, Y., Katagiri, H., Sakoda, H., Ogihara, T., Anai, M., Onishi, Y., Ono, H., Funaki, M., Inukai, K., et al. (2001). MKK6/3 and p38 MAPK pathway activation is not necessary for insulin-induced glucose uptake but regulates glucose transporter expression. J. Biol. Chem. *276*, 19800–19806.

Gao, J., Ye, H., and Serrero, G. (2000). Stimulation of adipose differentiation related protein (ADRP) expression in adipocyte precursors by long-chain fatty acids. J. Cell. Physiol. *182*, 297–302.

Hirsch, D., Stahl, A., and Lodish, H.F. (1998). A family of fatty acid transporters conserved from mycobacterium to man. Proc. Natl. Acad. Sci. USA *95*, 8625–8629.

Holm, C., Osterlund, T., Laurell, H., and Contreras, J.A. (2000). Molecular mechanisms regulating hormone-sensitive lipase and lipolysis. Annu. Rev. Nutr. *20*, 365–393.

Holman, G.D., and Sandoval, I.V. (2001). Moving the insulin-regulated glucose transporter GLUT4 into and out of storage. Trends Cell Biol. *11*, 173–179.

Hotamisligil, G.S. (2000). Molecular mechanisms of insulin resistance and the role of the adipocyte. Int. J. Obes. Relat. Metab. Disord. *24*, S23–27.

Hotamisligil, G.S., Peraldi, P., Budavari, A., Ellis, R., White, M.F., and Spiegelman, B.M. (1996). IRS-1-mediated inhibition of insulin receptor tyrosine kinase activity in TNF-alpha- and obesity-induced insulin resistance. Science *271*, 665–668.

Hube, F., and Hauner, H. (2000). The two tumor necrosis factor receptors mediate opposite effects on differentiation and glucose metabolism in human adipocytes in primary culture. Endocrinology *141*, 2582–2588.

Kahn, B.B. (1996). Lilly lecture 1995. Glucose transport: pivotal step in insulin action. Diabetes *45*, 1644–1654.

Kayali, A.G., Austin, D.A., and Webster, N.J. (2000). Stimulation of MAPK cascades by insulin and osmotic shock: lack of an involvement of p38 mitogen-activated protein kinase in glucose transport in 3T3-L1 adipocytes. Diabetes *49*, 1783–1793.

Man, M.Z., Hui, T.Y., Schaffer, J.E., Lodish, H.F., and Bernlohr, D.A. (1996). Regulation of the murine adipocyte fatty acid transporter gene by insulin. Mol. Endocrinol. *10*, 1021–1028.

Memon, R., Feingold, K., Moser, A., Fuller, J., and Grunfeld, C. (1998). Regulation of fatty acid transport protein and fatty acid translocase mRNA levels by endotoxin and cytokines. Am. J. Physiol. *274*, E210–217.

Peraldi, P., Hotamisligil, G.S., Buurman, W.A., White, M.F., and Spiegelman, B.M. (1996). Tumor necrosis factor (TNF)-alpha inhibits insulin signaling through stimulation of the p55 TNF receptor and activation of sphingomyelinase. J. Biol. Chem. *271*, 13018–13022.

Schaffer, J.E., and Lodish, H.F. (1994). Expression cloning and characterization of a novel adipocyte long chain fatty acid transport protein. Cell *79*, 427–436.

Stahl, A., Gimeno, R.E., Tartaglia, L.A., and Lodish, H.F. (2001). Fatty acid transport proteins: a current view of a growing family. Trends Endocrinol. Metab. *12*, 266–273.

Stahl, A., Hirsch, D.J., Gimeno, R., Punreddy, S., Ge, P., Watson, N., Kotler, M., Tartaglia, L.A., and Lodish, H.F. (1999). Identification of a small intestinal fatty acid transport protein. Mol. Cell *4*, 299–308.

Stump, D.D., Fan, X., and Berk, P.D. (2001). Oleic acid uptake and binding by rat adipocytes define dual pathways for cellular fatty acid uptake. J. Lipid Res. *42*, 509–520.

Tartaglia, L.A., Pennica, D., and Goeddel, D.V. (1993). Ligand passing: the 75-kDa tumor necrosis factor (TNF) receptor recruits TNF for signaling by the 55-kDa TNF receptor. J. Biol. Chem. *268*, 18542–18548.